

## Quantitative piezospectroscopy of neutral copper in germanium

E. H. Salib,\* P. Fisher, and P. E. Simmonds

*Department of Physics, The University of Wollongong, Wollongong, New South Wales 2500, Australia*

(Received 26 July 1984)

Experimental results of the optical-absorption spectrum of neutral copper impurity in germanium with and without an applied uniaxial compressive force  $\mathbf{F}$  are described. The zero-stress spectrum agrees with previous work and indicates that the absorption lines observed correspond to the excitation of one of the three bound holes to single-acceptor-like, higher-lying states. This is used as the basis of a model (described elsewhere) to explain the piezospectroscopic behavior of the spectrum observed with  $\mathbf{F}||\langle 100 \rangle$ ,  $\mathbf{F}||\langle 111 \rangle$ , and  $\mathbf{F}||\langle 110 \rangle$ ; this model is similar to that already exploited to describe the behavior of neutral group-II acceptors in germanium. The results obtained are much simpler than might be expected for such a complex system, although it has been shown that the antisymmetric product of three single-hole  $\Gamma_8(\bar{T}_d)$  ground states is itself a  $\Gamma_8(\bar{T}_d)$  state and not a multiplet as is the case for neutral group-II impurities. A detailed comparison between the results predicted by the symmetry analysis of the model permits the intensity parameters of some of the transitions to be determined and also deformation-potential constants of some of the energy states. The latter are found to be consistent with those for single-hole states in agreement with the model. However, several discrepancies remain between the model and the observations. A characteristic difference between the piezospectra of this impurity and the shallower group-III acceptors is that the intensities of the lower-energy  $G$  components increase with increasing stress whereas for a group-III impurity the higher-energy  $G$  components survive at large stress.

### I. INTRODUCTION

The optical spectroscopy of impurities in semiconductors is a valuable method for categorizing energy states of impurities and for also providing information about the host crystal. Extensive studies have been made of the Lyman series in absorption arising from impurities in silicon and germanium with and without external perturbations.<sup>1</sup> The classic spectra are those of the group-III and group-V impurities in these elemental semiconductors while some results have been reported for the group-II impurities in either their neutral or singly-ionized states. For example, such studies for these impurities in germanium have been made for Be,<sup>2,3</sup> Mg,<sup>3</sup> Zn,<sup>4-11</sup> and Hg.<sup>5,8,12,13</sup>

The present paper reports similar observations for the group-I impurity, neutral copper, in germanium,<sup>4,5,14-17</sup> the perturbations used being uniaxial compressive forces. The details of the group-theoretical analysis of the effect of uniaxial compression on the energy states of a substitutional triple acceptor in a group-IV semiconductor are presented elsewhere.<sup>16-18</sup> In this treatment the symmetries of the ground and excited states have been found by considering that each hole moves in the average field of the core and the other two holes. Thus, for example, the ground state is found to be the expansion of  $\{\Gamma_8 \times \Gamma_8 \times \Gamma_8\}$ , where  $\Gamma_8$  is the four-dimensional representation of the double group  $\bar{T}_d$ . Surprisingly this reduces to  $\Gamma_8$ ,<sup>16-19</sup> giving a significant simplification to the problem at least in terms of this model.

### II. EXPERIMENTAL PROCEDURE

The single-crystal copper-doped germanium samples were prepared by diffusing copper into the host at a

preselected temperature followed by a rapid quenching. Oriented samples of germanium were cut from ingots of essentially intrinsic material, ground roughly to size, copper plated, encapsulated in a fused quartz tube (either evacuated or filled with helium gas), heated to the desired temperature, held at that temperature for one hour, and then radiation quenched by dropping the capsule directly from the furnace into a Dewar of liquid nitrogen. This method is essentially that prescribed by Fuller *et al.*<sup>20</sup> The concentrations achieved for the different diffusion temperatures were determined using the results given by Fistul' *et al.*<sup>21</sup> Samples of different orientations, but required to have the same impurity concentration, were diffused at the same time in the same capsule. The doped samples were then prepared for the stress measurements by grinding and polishing these to an optical finish. The completed samples were typically about  $2 \times 5 \times 20$  mm<sup>3</sup> in size with a sufficient wedge along the length to suppress channeled spectra. The cross-sectional area of a sample was determined by direct measurement with a dial gauge and then compared with that obtained from measuring the length of the sample and its mass, using the known density of germanium.<sup>22</sup> The two estimates for the cross-sectional area agreed to better than 0.75%. The orientation of some of the samples was verified using the standard x-ray technique.

The general procedures for mounting and stressing the sample are described elsewhere.<sup>23,24</sup> Some improvement was made in the technique used to mount the sample.<sup>17</sup> For measurements at very low stresses, the pressure head of Ref. 23 was replaced by a platform on which were placed calibrated weights. Masses of up to 20 kg were used in this case. The pressure head itself was calibrated

against a proving ring.<sup>25</sup> The infrared spectrometer used to carry out the absorption measurements was comprised of a SPEX-1402 double monochromator<sup>26</sup> suitably equipped with source and sample optics all of which were flushed with dry air to remove atmospheric water vapor. The sample optics were arranged so that rotation of a single mirror permitted the monochromator to be used in either single or double mode, although in all the measurements to be described the latter was employed. During the course of the measurements, the calibration of the monochromator was found to remain constant as determined from atmospheric water-vapor lines.<sup>27</sup> A single interference filter<sup>28</sup> was found to be very efficient in suppressing unwanted higher-order radiation while a polyethylene pile-of-plates polarizer<sup>29</sup> was used in the stress measurements.

The detector was zinc-doped germanium<sup>30</sup> cooled with liquid helium in a modified MHD-3L Andonian cryostat,<sup>31</sup> the signal being chopped at 1.28 kHz and collected with a lock-in amplifier.<sup>32</sup> The output of the amplifier was processed by a digital voltmeter<sup>33</sup> which was interfaced to a Hewlett-Packard calculator,<sup>34</sup> a Data General Nova minicomputer,<sup>35</sup> or a Rockwell International AIM-65 microcomputer.<sup>36</sup> The data was ultimately stored on floppy discs and processed in the minicomputer equipped with a hard-copy plotter.<sup>37</sup> No smoothing or shape restoration of the data was deemed necessary since a sufficiently high signal-to-noise ratio could be obtained with a spectral slit width several times smaller than the width of the spectral lines of copper impurity in germanium. More details regarding the instrumentation and data collection and processing are given in Ref. 17.

### III. EXPERIMENTAL RESULTS AND DISCUSSION

In this section we present the results of the optical-absorption spectrum of copper impurity in germanium. The spectral region involved overlaps part of the strong lattice absorption of intrinsic germanium.<sup>38</sup> In order to obtain undistorted impurity spectra, it was found necessary to make a precise measurement of the lattice absorption of germanium and subtract this from the various impurity spectra.

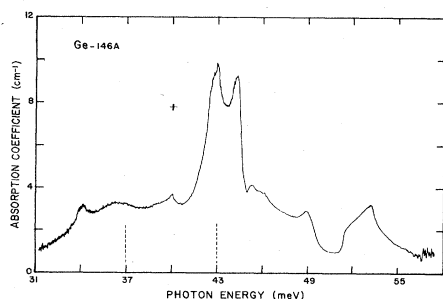


FIG. 1. Part of the lattice absorption spectrum of intrinsic germanium at liquid-helium temperature. The two vertical dashed lines define the range of most of the observations made on the spectrum of neutral copper in germanium. The spectral slit width is indicated at 40 meV.

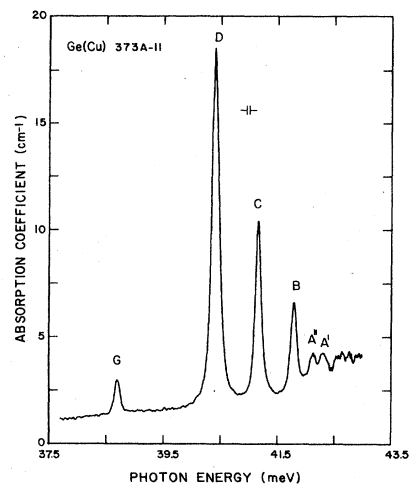


FIG. 2. Optical absorption spectrum of neutral copper impurity in germanium, lattice absorption subtracted. Liquid helium used as coolant. Copper diffused at 730°C corresponding to a concentration ( $N_{Cu}$ ) of substitutional copper of  $4.7 \times 10^{15} \text{ cm}^{-3}$  as estimated from Ref. 21. The spectral slit width is indicated at 41 meV.

#### A. Lattice absorption spectrum of germanium

The result of a precision measurement of the lattice absorption of germanium, near liquid-helium temperature, in the photon energy range of 31 to 55 meV is given in Fig. 1; an essentially intrinsic germanium sample was utilized. The spectral slit width used was the same as that employed in observing the impurity spectra in order that the lattice absorption could be subtracted as completely as possible. The dashed vertical lines in Fig. 1 define the range of the photon energies encountered in the present piezospectroscopic measurements.

#### B. Zero-stress spectrum of neutral copper in germanium

The Lyman absorption spectrum of neutral copper impurity in germanium is shown in Fig. 2 after subtraction of the lattice absorption. It is essentially the same as those previously reported<sup>4,5,14-16</sup> except that the  $A'''$  line observed by Butler and Fisher<sup>14</sup> has not been observed. The energies and energy spacings for the spectral lines of copper are given in Table I along with those reported by other workers as well as the corresponding average energy spacing for group-III impurities in germanium. An estimate of the ionization energy is also given in the table; this has been obtained using the procedure given in Ref. 1. It is clear from Table I that the spacings of the excited states of copper and those of the single-hole acceptors in germanium are the same, implying that the observed transitions for neutral copper are those of single-hole excitations. A comparison of the average relative intensities of the  $B$ ,  $C$ ,  $D$ , and  $G$  lines for three different samples with those of the single-hole acceptor gallium<sup>39</sup> and a recent calculation<sup>40</sup> is given in Table II. From the results in Tables I and II it would appear that the effective-mass formalism is an adequate description of the excited states of the triple-hole system.

TABLE I. Energies and energy spacings (in meV) of spectral lines of neutral copper in germanium.

Line	Present work		Group-III average value		Other workers		
	Energy	Spacing relative to <i>D</i> line	Ref. 1	Ref. 4	Ref. 5	Ref. 14	Ref. 15
<i>G</i>	38.67±0.01	1.70±0.02	1.69	38.67	38.61		
<i>D</i>	40.37±0.01	0	0	40.40	40.33	40.39	40.35
<i>C</i>	41.12±0.01	0.77±0.02	0.75	41.12	41.06	41.13	41.10
<i>B</i>	41.76±0.01	1.39±0.02	1.39	41.79	41.76	41.75	41.72
<i>A''</i>	42.07±0.04	1.70±0.05	1.73			42.08	42.13
<i>A'</i>	42.27±0.05	1.90±0.06	1.87			42.27	42.35
<i>E<sub>I</sub></i> <sup>a</sup>	43.25±0.01			43.28	43.21	43.27	43.23

<sup>a</sup>The ionization of energy  $E_I$  is calculated assuming a binding energy of 2.88 meV for the final state of line *D* (see Ref. 1).

It is worth noting that one set of samples was initially diffused at 650°C. These yielded none of the characteristic neutral copper absorption lines of Fig. 1 but did exhibit significantly larger background absorption than that obtained for samples diffused at 700°C and above. From the results given by Fistul' *et al.*<sup>21</sup> it is expected that the *D* line for the 650°C sample should be at least as large as the *G* line of the 730°C sample whose spectrum is shown in Fig. 1. Note that  $N_A$  for a sample diffused at 650°C is predicted to be  $1.27 \times 10^{15} \text{ cm}^{-3}$  by extrapolation of the data given in Ref. 21. Neither this aspect nor the origin of the large background is understood, but these have not been pursued. It might be conjectured that the copper forms a larger concentration of complexes at the lower diffusion temperature producing copper-related centers with ionization energies less than that of the substitutional neutral copper. Copper-related complexes in germanium have been observed by Haller *et al.*<sup>15</sup> and possibly by Butler and Fisher.<sup>14</sup>

### C. Effect of uniaxial stress

#### 1. Applied force along a $\langle 100 \rangle$ axis

*a. Stress dependence at a fixed temperature.* The behavior of the optical-absorption spectrum of neutral copper impurity in germanium for a compressive force  $F \parallel \langle 100 \rangle$  is shown in Figs. 3–7 for a sample quenched from 730°C. The radiation is polarized either parallel or perpendicular to  $F$ . In Figs. 3–5 the structure designated  $\text{H}_2\text{O}$  is the residual of the strong atmospheric water-vapor

TABLE II. Relative intensities of absorption lines of acceptors in germanium.

Line	Neutral copper <sup>a</sup>	Gallium <sup>b</sup>	Theory <sup>c</sup> (gallium)
$I(D)/I(B)$	4.70±0.30	5.47±0.50	13.33
$I(D)/I(C)$	2.42±0.07	1.06±0.10	2.40
$I(D)/I(G)$	13.2±1.10	11.58±1.15	63.16

<sup>a</sup>The intensity of the *D* line for a sample diffused at 730°C is  $4.05 \pm 0.35 \text{ cm}^{-1} \text{ meV}$ .

<sup>b</sup>Reference 39.

<sup>c</sup>See Table I in Ref. 40, where the *C* and *B* lines are taken to be a  $\Gamma_8^+ \rightarrow \Gamma_7^- + \Gamma_8^-$  transition and a  $\Gamma_8^+ \rightarrow \Gamma_8^-$  transition, respectively.

absorption line at  $\sim 37.6 \text{ meV}$  ( $\sim 303 \text{ cm}^{-1}$ ).<sup>27</sup> The "quench temperature" for this sample was chosen so that the *B*, *C*, and *D* lines could be studied with optimum-absorption coefficients. The *G* line, weak at small stresses, was further studied using a sample quenched from 800°C which gave rise to a *G* line approximately 3 times more intense than that of the 730°C samples. Data for the 800°C sample are not shown but were very similar to those of the 730°C sample.<sup>17</sup> Figure 6 illustrates the stress dependence of the energies of the various stress-induced components, the data for stresses  $< 0.3 \text{ kbar}$  being obtained with calibrated weights whereas those above were obtained using the pressure head.<sup>23</sup> The solid lines in the figure represent least-squares polynomial fits to the most reliable of the data points excluding the zero-stress energy of each component. The zero-stress energies of the various lines are shown as square data points.

The following remarks can be made regarding the general features of the spectra. First, the stress-induced spectra are much simpler than one may expect for such a complex system. The *C*, *D*, and *G* lines split into four

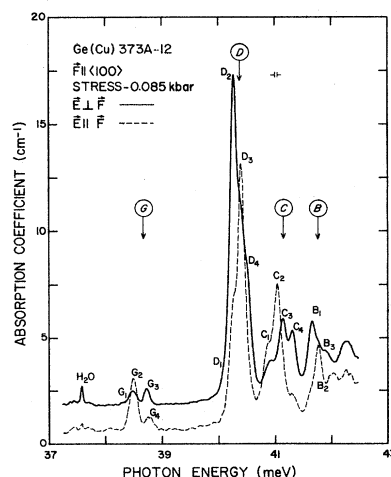


FIG. 3. Effect of a compressive force,  $F$ , on the spectrum of neutral copper in germanium with  $F \parallel \langle 100 \rangle$  for a stress of 0.085 kbar. Liquid helium used as coolant.  $E$  is the electric field of the radiation. Copper diffused at 730°C;  $N_{\text{Cu}} = 4.7 \times 10^{15} \text{ cm}^{-3}$ . The encircled letters with their associated arrows designate the zero-stress absorption lines. The spectral slit width is indicated at 41 meV.

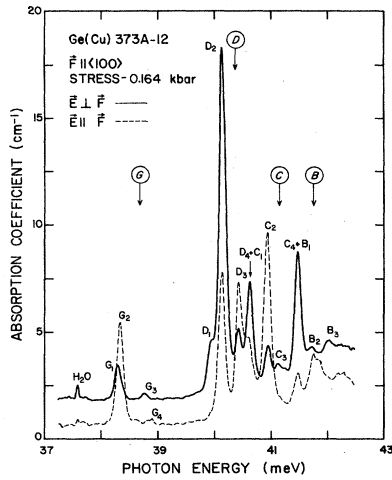


FIG. 4. Same as for Fig. 3 but for a stress of 0.164 kbar.

components which is similar to the case of the  $D$  and  $G$  lines of single-hole acceptors.<sup>9,10,41,42</sup> Also, the polarization and relative intensities of the stress-induced components of the  $D$  line are remarkably similar to those observed for thallium in germanium,<sup>41</sup> although this similarity must be qualified as will be discussed later. However, the  $G$  line behaves in a fashion different to that of the single acceptor. The above studies of the  $D$  and  $G$  lines of single acceptors in germanium have confirmed the fact that these lines correspond to  $\Gamma_8 \rightarrow \Gamma_8'$  transitions. It should be pointed out, though, that the Zeeman measurements of Soepangkat and Fisher<sup>43</sup> for boron in germanium show that the behavior of the  $G$  line under the effect of external magnetic field is quite different to that of the  $D$  line. Secondly, the higher-energy stress-induced components of the  $B$ ,  $C$ , and  $D$  lines have essentially disappeared at intermediate stresses, possibly due to their upper substates being in resonance with the free-hole states of the stress-split valence band,<sup>44</sup> which may also be the reason why all the  $B$  and  $D$  components have vanished at the highest stress. Thirdly, the stress dependence of the intensity of most of the stress-induced components is very dramatic; this will be discussed later in detail. At stresses higher than about 0.6 kbar, the component designated as

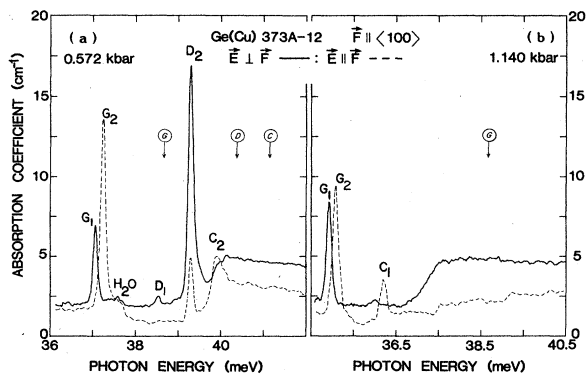


FIG. 5. Same as for Fig. 3 but at stresses of (a) 0.572 and (b) 1.140 kbar.

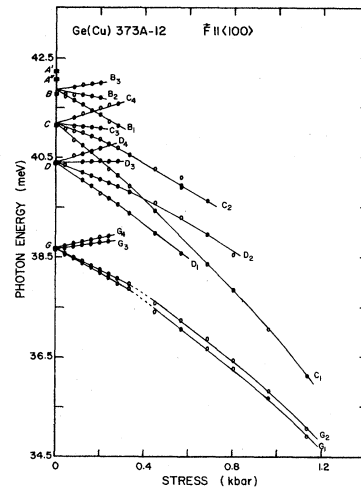


FIG. 6. Stress dependence of the energies of the components of the  $B$ ,  $C$ ,  $D$ , and  $G$  lines of copper-doped germanium for  $F \parallel \langle 100 \rangle$ . Calibrated weights used for stresses  $< 0.3$  kbar, a pressure head used for stresses greater than this (see text).

$C_1$  is found to grow in intensity with stress and was thought originally to be a new line, but from Fig. 6 one can identify this component either as a  $C_1$  component or a transition to a combined final substate of the original final substates of the  $C_1$  and  $D_1$  components. It will be seen later that the growth of this component may account for the rapid decrease at higher stress of the intensity of the  $G_2$  component. Fourthly, there is no clear evidence of interaction between final substates of the  $G$  components and the optical phonon of germanium at 37.2 meV.<sup>45,46</sup> This presumably means that the acceptor-phonon coupling for the copper states in germanium is very weak. Finally, it has to be borne in mind that there is some residual structure due to some water-vapor absorption lines other than the one mentioned above, and this may well be a source of errors in the determination of the energies of

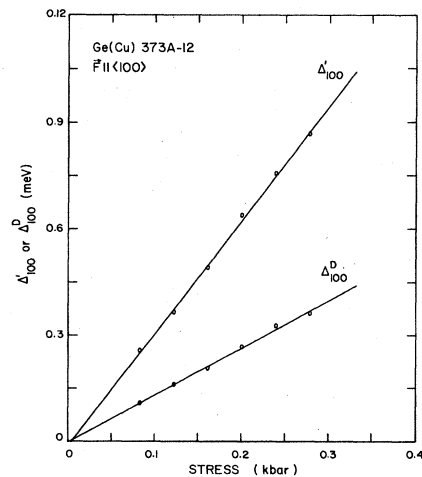


FIG. 7. Stress dependence of the splitting of the ground state ( $\Delta'_{100}$ ) and the splitting of the single-hole excited state of the  $D$  line ( $\Delta''_{100}$ ) for  $F \parallel \langle 100 \rangle$ . Data obtained from the stress dependence of the  $D$  components of copper impurity in germanium.

TABLE III. Splittings (in meV) of the ground and excited states of neutral copper in germanium for  $\mathbf{F}||\langle 100 \rangle$ . (All entries are to be multiplied by  $|T|$ ;  $T$  is the stress in kbar.)

Splittings		Sample	No. 12 (730°C)	No. 8 (730°C)	No. 2A (800°C)
$\Delta'_{100}$	$\frac{1}{2}[(\epsilon_{G_4} - \epsilon_{G_2}) + (\epsilon_{G_3} - \epsilon_{G_1})]$		3.04±0.03	3.27±0.10	3.21±0.04
	$\frac{1}{2}[(\epsilon_{D_4} - \epsilon_{D_2}) + (\epsilon_{D_3} - \epsilon_{D_1})]$		3.14±0.05		
	$\frac{1}{2}[(\epsilon_{C_4} - \epsilon_{C_2}) + (\epsilon_{C_3} - \epsilon_{C_1})]$		3.16±0.05		
	$(\epsilon_{B_3} - \epsilon_{B_1})$		3.20±0.11		
$\Delta^G_{100}$	$(\epsilon_{G_4} - \epsilon_{G_3})$		0.34±0.02	0.57±0.07	
	$(\epsilon_{G_2} - \epsilon_{G_1})$		0.35±0.03	0.52±0.10	
	$\frac{1}{2}[(\epsilon_{G_4} - \epsilon_{G_3}) + (\epsilon_{G_2} - \epsilon_{G_1})]$		0.34±0.03	0.55±0.08	0.50±0.04
$\Delta^D_{100}$	$\frac{1}{2}[(\epsilon_{D_4} - \epsilon_{D_3}) + (\epsilon_{D_2} - \epsilon_{D_1})]$		1.32±0.03		

the weak stress-induced components as they cross over one of these lines.

On the basis of the self-consistent-field approximation for triple acceptors in group-IV semiconductors,<sup>16-19</sup> it has been shown (as already mentioned) that the ground state is a  $\Gamma_8$  state in agreement with statements made by others.<sup>15,47</sup> Accordingly, one would expect such a state to split into two Kramers-degenerate substates under uniaxial compression. It is also predicted<sup>16-18</sup> that the final states of the  $D$  and  $G$  lines are each represented by  $\{\Gamma_8 \times \Gamma_8\} \times \Gamma'_8$ , a 24-fold degeneracy. Further, the model predicts that for  $\mathbf{F}||\langle 100 \rangle$  each of these two lines should split into four components, as is the case (see Fig. 6), from which one can obtain both the ground- and excited-state splittings. It should be noted that each component is predicted to be composed of two transitions of equal energy,<sup>16-18</sup> since for this model an important simplifying assumption is that the ground-state splitting,  $\Delta'_{100}$ , also recurs in the excited state.

Experimentally, one is searching for a splitting which is common to the components of the various lines. This common splitting should then be  $\Delta'_{100}$ . The common splitting within the components of a given line will be the excited-state splittings appropriate to that line; this is designated as  $\Delta^X_{100}$ , where  $X$  denotes  $B$ ,  $C$ ,  $D$  or  $G$ . The results obtained for these splittings are given in Table III. In this table the components of a given line used to determine the splittings defined in the first column are given in the second column while data for three different samples<sup>17</sup> have been included. Shown in Fig. 7 is the stress dependence of the splitting of the ground state as determined from the  $D$  components along with the splitting of the excited state of the  $D$  line for sample No. 12 (730°C) (see Table III). The solid lines in Fig. 7 are linear least-squares fits through the data points. Similar results are obtained for the  $G$  line. The average values of the ground and excited states splittings are found to be

$$\Delta'_{100} = (3.17 \pm 0.08) |T| \text{ meV},$$

$$\Delta^G_{100} = (0.46 \pm 0.11) |T| \text{ meV},$$

$$\Delta^D_{100} = (1.32 \pm 0.03) |T| \text{ meV},$$

where  $T$  is the stress in kbars.

The stress dependence of the intensity of a given line component has been estimated from the various spectra. The results obtained for the  $D$  and  $G$  lines for  $\mathbf{F}||\langle 100 \rangle$  are shown in Figs. 8 and 9, respectively. These illustrations are for  $\mathbf{E}$ , the electric field of the radiation, polarized perpendicular to  $\mathbf{F}$  (designated  $E_{\perp}$ ) and  $\mathbf{E}$  parallel to  $\mathbf{F}$  (designated  $E_{\parallel}$ ). Note that two different samples have been used to obtain these data. Similar results to those shown for the  $G$  components in Fig. 9 were obtained for the 730°C sample of Fig. 8. The data used are those obtained at small stresses using weights. The intensity of each component has been determined by "weighing the area" under its absorption profile. Each component has been "peeled off" from the other components; this is done graphically.<sup>11,48</sup> The background due to the impurity absorption (not the lattice absorption) for each spectrum at different stress was chosen as a smooth curve close to the "deepest valley" between the overlapping components, taking into account the shape of the background at very low stress as a guide for a realistic choice. The solid lines through the data points in Figs. 8 and 9 are included as an aid to the eye and are drawn through the most reliable data points. There are several probable

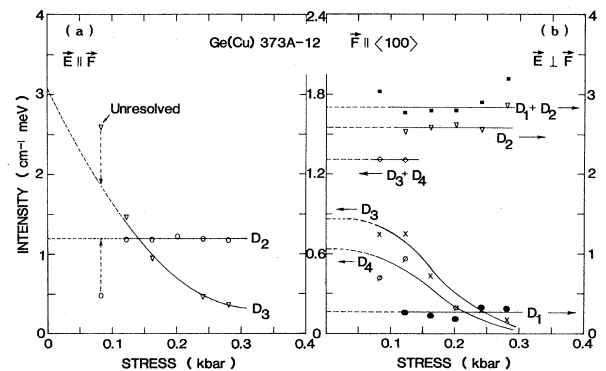


FIG. 8. Stress dependence of the intensities of the  $D$  components of copper in germanium for  $\mathbf{F}||\langle 100 \rangle$  at a fixed temperature for the sample of Figs. 3-5.

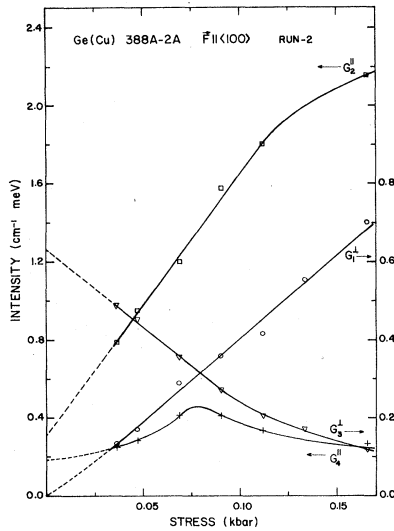


FIG. 9. Stress dependence of the intensities of the components of the  $G$  line of copper in germanium for  $F||\langle 100 \rangle$  at a fixed temperature. Copper diffused at  $800^\circ\text{C}$ ;  $N_{\text{Cu}} = 1.32 \times 10^{15} \text{ cm}^{-3}$ .

sources of error in these estimates. First, the small absorption due to the residual water-vapor absorption cannot be taken into account when this is obscured by the component whose intensity is being determined. Secondly, if the sample temperature changes with stress, as is probably the case at small stresses, then the low-stress intensity data would be somewhat unreliable. The third, and probably the most important, uncertainty is the somewhat arbitrary choice of the background and the graphical method of separating overlapping and partially resolved components.

For the  $D$  line, the fact that of the four components observed, the two for  $E||$  are intermediate in energy, leads to the conclusion that the order of the stress-induced substates of the ground state is the same as that of the stress-induced single-hole final substates as is shown in Fig. 1 of Ref. 16. Thus, we have only two possible arrangements depending upon which of the ground substates,  $\{\Gamma_7 \times \Gamma_7\} \times \Gamma_6$  or  $\{\Gamma_6 \times \Gamma_6\} \times \Gamma_7$ , is the lower in energy. In Fig. 1 of Ref. 16, the ordering of the substates of the ground state and those of the  $\{\Gamma_8 \times \Gamma_8\} \times \Gamma_8'$  excited state have been chosen to be consistent with the single-acceptor scheme for the  $D$  line. For example, if the symmetry of the lower-energy substate of the ground state of the single acceptor is  $\Gamma_7$ ,<sup>9,10,42</sup> then the substate represented by  $\{\Gamma_7 \times \Gamma_7\} \times \Gamma_6$  would be the lower substate of the triple acceptor. Since an observed component is predicted to be comprised of two transitions, one originating from the lower and the other from the upper ground substate, in what follows these will be designated by the subscripts  $l$  and  $t$ , respectively. For example,  $D_{1l}$  represents that transition contributing to  $D_1$  arising from the lower ground substate. The notable feature for the present spectra is that the intensities of the high-energy components decrease with increasing stress whereas the lower-energy components, although showing little change in intensity at

low stresses (see Fig. 8) are the components which survive at moderate stresses (see Fig. 6). This behavior is contrary to that which has been observed for the case of single acceptors.<sup>9,10,42</sup> This suggests for copper that the low-energy components are each comprised of pairs of transitions such that the one arising from the lower ground state is dominant. The other notable feature is that the intensity of  $D_2$  stays constant up to a stress of 0.3 kbar (see Fig. 8). This could be explained, for example, if the effect of the thermal population and depopulation with stress of  $D_{2l}$  and  $D_{2t}$ , respectively, is balanced by the interaction of the final substates of the  $D$  line with those of the other lines. This point will be returned to again when discussing the intensity variations of the various components with temperature. The relative intensities of  $D_2^{\parallel}$  and  $D_3^{\parallel}$ , predicted from the model are<sup>16-18</sup>

$$I(D_2^{\parallel}):I(D_3^{\parallel})::(\frac{1}{2}-v_D):(\frac{1}{2}+v_D),$$

where  $I(X_i)$  is defined to be the intensity of the  $i$ th component of the  $X$ th line and  $v_D$  is one of the two intensity parameters demanded by symmetry<sup>49</sup> which specifies the relative intensities of the components of the  $D$  line. From the extrapolated values of the intensities of  $D_2^{\parallel}$  and  $D_3^{\parallel}$  to zero strain in Fig. 8(a), one obtains

$$I(D_2^{\parallel}):I(D_3^{\parallel})::1.19:3.05::0.28:0.72,$$

giving a value of  $0.22 \pm 0.04$  for  $v_D$  where the estimated error in  $I(D_2^{\parallel})$  or  $I(D_3^{\parallel})$  is about  $\pm 10\%$ . Note that in the extrapolation of the  $I(D_2^{\parallel})$  data in Fig. 8(a), the datum point at 0.085 kbar was excluded and the difference between its value and the extrapolation of  $I(D_2^{\parallel})$  subtracted from the corresponding datum point of  $I(D_3^{\parallel})$  to obtain a point to be used in the extrapolation of  $I(D_3^{\parallel})$  [see Fig. 8(a)]. This was possible since  $D_2^{\parallel}$  and  $D_3^{\parallel}$  are the only components for  $E||F$ . If we substitute the above value of  $v_D$  into the expression for the relative intensities of  $(D_1^{\perp} + D_2^{\perp})$  and  $(D_3^{\perp} + D_4^{\perp})$ , one obtains<sup>16-18</sup>

$$I(D_1^{\perp} + D_2^{\perp}):I(D_3^{\perp} + D_4^{\perp})::\frac{1}{2}(1+v_D):\frac{1}{2}(1-v_D) \\ ::0.61:0.39,$$

which is in good agreement with the extrapolated values of the  $(D_1^{\perp} + D_2^{\perp})$  and  $(D_3^{\perp} + D_4^{\perp})$  data for zero strain obtained from Fig. 8(b), viz., 0.68:0.32. This result supports the prediction made earlier about the relative ordering of the ground and excited substates of the  $D$  line. A rough estimate can now be obtained for the value of the second intensity parameter  $u_D$ ,<sup>49</sup> by utilizing the intensity of either the  $D_1^{\perp}$  or  $D_4^{\perp}$  component and the sum of the intensities of all the  $D$  components for  $E_{\perp}$  since<sup>16-18</sup>

$$I(D_1^{\perp}) = I(D_4^{\perp}) = \frac{3}{8} u_D I(D_1^{\perp} + D_2^{\perp} + D_3^{\perp} + D_4^{\perp}).$$

From the extrapolated value of  $I(D_1^{\perp})$  at zero stress, in Fig. 8(b), it is deduced that  $u_D = 0.2$ . The value obtained in the same manner from  $I(D_4^{\perp})$  is 0.4, giving an average value of 0.3 for  $u_D$ .

In general, as has been seen the agreement between the theory and the experimental results for the  $D$  line, for  $F||\langle 100 \rangle$ , is very good; this is not the case for the behavior of the  $G$  line even though the symmetry of the

final state of the  $G$  line is believed to be the same as that of the  $D$  line. The observation of four stress-induced components for the  $G$  line is in agreement with the prediction that this line is a  $\Gamma_8 \rightarrow \{\Gamma_8 \times \Gamma_8\} \times \Gamma'_8$  transition. The polarization of these components, however, is not understood since of the two  $E_{||}$  components  $G_2^{\parallel}$  is of intermediate energy while  $G_4^{\parallel}$  is an extreme energy component (see Figs. 3–6); this is contrary to the predictions, as may be appreciated from the above discussion for the  $D$  line. There are dramatic stress-induced variations in the intensities of the  $G$  components, those of the low-energy components  $G_1$  and  $G_2$  being greatly enhanced (at least up to moderate stresses) while the high-energy components  $G_3$  and  $G_4$  fall to zero. In Fig. 9 (and for the 730°C sample) at low stress, the rate at which  $G_3^{\parallel}$  decreases with stress appears to be about the same as the rate at which  $G_1^{\parallel}$  increases. This may be an example of the stress interaction of the substates within a given manifold of final states of the type described by Duff *et al.*,<sup>11</sup> whereas at higher stresses the change in intensity might be due to interactions between final substates belonging to different manifolds as first pointed out by Chandrasekhar *et al.*,<sup>50</sup> and/or thermal depopulation effects. The first of these interactions is attributed to the impurity atom not substituting exactly for the host atom but moving off the  $T_d$  site while the second type is due to strain-induced mixing of substates of the same symmetry. Both of these interactions were investigated<sup>11,50</sup> in the spirit of a linear expansion of the strain potential in terms of the strain. "Off-site interaction" has not been taken into account in the present model.<sup>16–18</sup> It is also observed that the stress-induced  $G$  components are totally polarized. For instance, at moderate stress and higher,  $G_1$  and  $G_3$  are observed for  $E_{\perp}$  alone while  $G_2$  and  $G_4$  only occur for  $E_{||}$ . In addition, the intensities of  $G_1^{\parallel}$  and  $G_2^{\parallel}$  extrapolated to zero stress (see Fig. 9) are very small.

In view of the above and the predicted relative intensities for  $\Gamma_8 \rightarrow \{\Gamma_8 \times \Gamma_8\} \times \Gamma'_8$  components, it is clear that, unlike the case of the  $D$  line, no satisfactory assignment can be obtained for the  $G$  components and thus no values for  $u_G$  and  $v_G$  can be deduced from the results for  $F_{||}\langle 100 \rangle$ .

The complexity of the interactions which may be taking place is suggested by the result that the sum of the intensities of  $C_2^{\parallel}$ ,  $D_3^{\parallel}$ , and  $G_2^{\parallel}$ , as a function of stress, is constant at low values of stress (see Fig. 31 of Ref. 17). This may imply that interactions are occurring among final substates of all three lines  $C$ ,  $D$ , and  $G$ . A similar result is obtained for components polarized with  $E_{\perp}$ . It should be noted that, although the sum of these components is almost constant with stress, this does not imply a conservation of intensity for these transitions since many other transitions are omitted from the summation.

*b. Temperature dependence at fixed stress.* In addition to any interactions which may be taking place, there will be the effect of thermal depopulation on the intensities of the various components. This is a consequence of the variation of the ground-state splitting with stress. In order to separate these effects from others such as interactions, several measurements have been made at different sample temperatures with a fixed stress; the different tem-

peratures were achieved by winding a heater onto the tail of the stress centerpiece.<sup>17</sup> The stress was chosen to be high enough to ensure a sufficiently large ground-state splitting for observable changes in the thermal populations of the two ground substates for the temperature variation available. Figure 10 illustrates the effect on the spectrum at different heating currents (the temperature of the sample was not measured) for  $F_{||}\langle 100 \rangle$ ,  $E_{||}F$ , and for a stress of 0.268 kbar. Similar results are obtained for  $E_{\perp}F$  and for other samples, and the intensities of the various components as a function of the square of the heating current have been determined. A typical result is shown in Fig. 11 for the  $G$  components at a stress of 0.227 kbar for a different sample from that of Fig. 10. In summary, for the  $D$  components at 0.268 kbar,  $D_1$  and  $D_2$  decrease in intensity, while  $D_3$  increases with increasing temperature; the behavior of  $D_4$  was not determined since its energy was close to that of  $C_2$  at this stress.

Recalling that on the model being used to describe this acceptor each component is composed of two transitions, one from each substate of the ground state, it is clear that the effect of the thermal depopulation on the intensity of the observed components need not be as simple as it is for the case of single acceptors where each component corresponds to a transition from only one of the ground-state substates. Thus, if for a given component, the transition from the lower ground-state sublevel is more probable than for its partner from the upper ground-state sublevel, an increase in temperature at a given stress will result in an overall decrease in the intensity of the component as the upper ground-state sublevel becomes more populated at the expense of the lower and *vice versa*. From the results obtained, for example, for the  $D_2^{\parallel}$  component, which very clearly decreases in intensity with increasing temperature (see Fig. 10), it is deduced that  $I(D_{2l}^{\parallel})$  is larger than that of  $I(D_{2t}^{\parallel})$  at the stress employed. This is contrary, however, to the predictions of the model at zero stress<sup>16–18</sup> for which  $I(D_{2l}^{\parallel})$  is calculated to be  $\frac{1}{2}I(D_{2t}^{\parallel})$ . When similar comparisons are made for the remaining  $D$

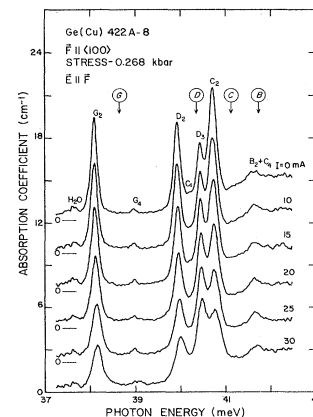


FIG. 10. Effect of temperature on the stress-induced components of the absorption spectrum of copper impurity in germanium (lattice absorption subtracted) for  $F_{||}\langle 100 \rangle$ ,  $E_{||}F$ , and at a stress of 0.268 kbar. The symbol  $I$  denotes the heater current. Copper diffused at 730°C;  $N_{Cu} = 4.7 \times 10^{15} \text{ cm}^{-3}$ .

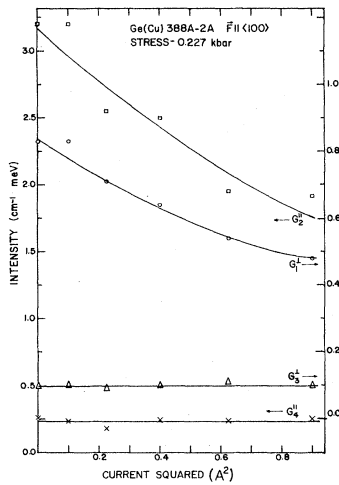


FIG. 11. Intensities of the components of the  $G$  line of copper impurity in germanium as a function of the square of the heater current at a stress of 0.227 kbar for a sample containing copper diffused at  $800^\circ\text{C}$ , for  $F \parallel \langle 100 \rangle$ .  $N_{\text{Cu}} = 1.32 \times 10^{16} \text{ cm}^{-3}$ .

components the same conclusion is reached. No consistent reordering of the substates of the ground and excited states rectifies this discrepancy. This apparent change in these relative magnitudes with stress for the  $D$  components suggests that interactions may be taking place between the final substates of these components and those of other lines. Note that in the model being used, no mixing<sup>11,50</sup> between the final substates has been included. Parenthetically, it might also be noted that if mixing were included the final substates of the two transitions making up a given component might undergo different interactions with adjacent substates thus leading to broadening or even splitting of the component. Such an effect has not been observed for any of the stress-induced components.

If the thermal depopulation is the only mechanism involved in the observed intensity variations with stress for the components of a given line, then it would be intuitively expected that the changes in intensity with increasing temperature would be opposite to those changes observed with increasing stress. Thus, for example, since the  $D_2^{\frac{1}{2}}$  and  $D_1^{\frac{1}{2}}$  components decrease with temperature, these would be expected to increase with stress. Nevertheless, from Figs. 8(a) and 8(b) it appears as if  $I(D_2^{\frac{1}{2}})$  and  $I(D_1^{\frac{1}{2}})$  are constant with stress. A similar but opposite effect occurs for  $G_3^{\frac{1}{2}}$  and  $G_4^{\frac{1}{2}}$  in that these stay constant with increasing temperature (see Fig. 11), although the behavior of  $G_4^{\frac{1}{2}}$  is not that well determined since it is weak. This suggests that each of the  $D_2$ ,  $G_3$ , and  $G_4$  components has an intensity behavior dictated by a mechanism other than that of thermal depopulation. The behavior of  $I(D_3)$ ,  $I(G_1)$ , and  $I(G_2)$  with stress (see Figs. 8 and 9) is in qualitative agreement with the temperature dependence of these components (see Figs. 10 and 11). However, since no attempt has been made to calibrate the sample temperature as a function of heating current, it was not possible to separate quantitatively the effects of the thermal depopulation from those of other mechanisms.

## 2. Applied force along a $\langle 111 \rangle$ axis

The spectrum for  $F \parallel \langle 111 \rangle$  is shown in Figs. 12 and 13 for a sample quenched from  $730^\circ\text{C}$ . Figure 14 illustrates the stress dependence of the energies of the various components of the  $B$ ,  $C$ ,  $D$ , and  $G$  lines. Another sample, quenched from  $800^\circ\text{C}$  to enhance the  $G$  line, gave almost identical results for both the energy and intensity dependence of the  $G$  components as those shown in Figs. 12–14. In Fig. 14 the solid lines are aids to the eye except for the  $G$  components for which these are linear least-squares fits for stress up to the data points distinguished by the arrow. In this figure the solid line through the data obtained at higher stresses for  $G_1$  is an extrapolation of the linear least-squares fit established for the low stress data. In addition, the linear part of the solid line drawn through the higher stress data of  $G_2$  is a linear least-squares fit.

The  $G$  line splits into at least two components  $G_1$  and  $G_2$ . The behavior of  $G_2$  is very striking; it exhibits a linear increase in energy at low stress, a significant non-linearity at moderate stress (causing its energy to decrease to less than that of the original line), and again becomes linear at high stress but now decreasing in energy with stress following, apparently, the same stress dependence as  $G_1$ .

At low stress, in contrast to the  $G$  line, the other lines are unaffected except for a very small shoulder on the  $C$  line, designated  $C_1$  in Fig. 12. It is not until a stress is attained at which  $G_2$  starts exhibiting its nonlinear behavior that any noticeable effect occurs for the other lines. Of the  $B$ ,  $C$ , and  $D$  lines, the most significant behavior is the splitting of the  $D$  line into two components, of which  $D_2$  is relatively weak, and the fact that, at high stress, the strong  $C$  and  $D$  components,  $C_2$  and  $D_1$ , have essentially the same stress dependence as  $G_1$  and  $G_2$ .

The intensity of the  $G_2$  component undergoes a dramatic change with stress. For example, at low stress  $G_2^{\frac{1}{2}}$  is initially much weaker than  $G_1^{\frac{1}{2}}$ , the intensity of the latter showing virtually no change with stress, whereas at the largest stress  $G_2^{\frac{1}{2}}$  is stronger than  $G_1^{\frac{1}{2}}$ . The rapid

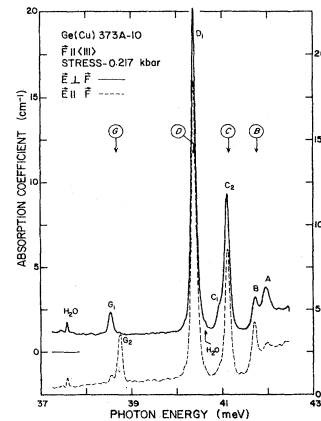


FIG. 12. Effect of a  $\langle 111 \rangle$  compressive force on the absorption spectrum of neutral copper impurity in germanium for a stress of 0.217 kbar. Liquid helium used as coolant. Copper diffused at  $730^\circ\text{C}$ ;  $N_{\text{Cu}} = 4.7 \times 10^{15} \text{ cm}^{-3}$ .

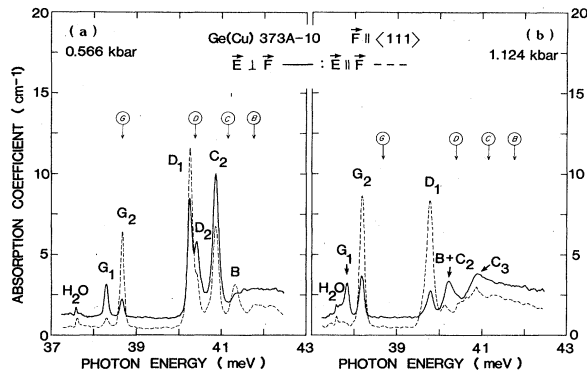


FIG. 13. Same as Fig. 12 but at stresses of (a) 0.566 and (b) 1.124 kbar.

change in intensity of  $G_2^{\perp}$  goes hand in hand with the nonlinear behavior of its energy. The intensity of  $G_2^{\parallel}$  is significantly larger than that of  $G_1^{\parallel}$  and behaves essentially like  $G_2^{\perp}$ .

The dramatic enhancement in the intensity of the  $G_2$  components is accompanied by a corresponding decrease in the intensity of the  $D$  line. The nonlinear behavior of both the  $D$  and  $G$  components and the change in their intensities with stress, suggest that strong interactions are taking place amongst their associated substates, as already indicated in the case of  $F_{\parallel}\langle 100 \rangle$ . A similar effect has been reported previously<sup>10,11</sup> for the case of singly-ionized zinc in germanium and recently observed for gallium in germanium.<sup>42</sup>

According to the model being used,<sup>16-18</sup> it is predicted that a common splitting should occur among the components of the various lines. As has been seen, such a common splitting is observed for the case of  $F_{\parallel}\langle 100 \rangle$ . In Fig. 14 no such splitting can be found amongst the components of the various lines up to the highest stress used, although the spacing of  $C_1$  and  $C_2$  is comparable to that of  $G_1$  and  $G_2$  at low stress. It should be noted, however, that the  $C_1$  component is extremely weak even when observed, moreover, at moderate stress, these two spacings ( $\epsilon_{G_2} - \epsilon_{G_1}$  and  $\epsilon_{C_2} - \epsilon_{C_1}$ ) are not equal. In addition, it is surprising that there is no splitting common to the  $D$  and  $G$  lines particularly as these two transitions are predicted to be of the same type. In fact, the  $D$  line exhibits little or

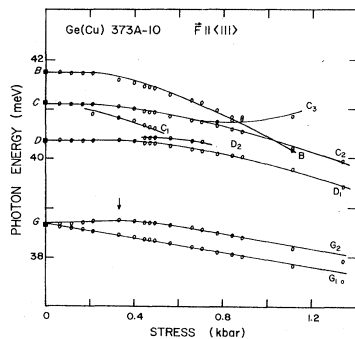


FIG. 14. Stress dependence of the energies of the components of  $B$ ,  $C$ ,  $D$ , and  $G$  lines of neutral copper impurity in germanium for  $F_{\parallel}\langle 111 \rangle$  for the sample of Figs. 12 and 13.

no splitting even at the highest stress used. The possibility that some of the  $D$  components are missing appears to be ruled out when the value of  $u_D (=0.3)$  obtained for  $F_{\parallel}\langle 100 \rangle$  is used to predict the relative intensities of the various  $D$  components<sup>17,18</sup> for  $F_{\parallel}\langle 111 \rangle$ . The above information strongly suggests that neither the  $\Gamma_8$  ground state nor the final state of the  $D$  line split for  $F_{\parallel}\langle 111 \rangle$ , i.e.,  $\Delta'_{111} = \Delta^D_{111} = 0$ . The deduction that  $\Delta^D_{111} = 0$  is in complete accord with results obtained experimentally for single-hole acceptors.<sup>7,9,10,41,42</sup> It should be mentioned that Haller *et al.*<sup>51</sup> have observed no ground-state splitting for some acceptor complexes in germanium for  $F_{\parallel}\langle 111 \rangle$ . This has been explained in terms of the "dynamic tunneling model" which predicts that the ground state of such an acceptor complex, at zero stress, is not a  $\Gamma_8$  state, but a Kramers doublet. This model is supported by a lack of splitting of the ground state for  $F_{\parallel}\langle 100 \rangle$  as well, which is not so in the present case.

In Fig. 15 the energy difference,  $\epsilon_{G_2} - \epsilon_{G_1}$ , designated  $\Delta^G_{111}$ , is plotted as a function of stress for the 800°C sample; an almost identical result is obtained from the data of Fig. 14. The straight line represents a linear least-squares fit to the data up to 0.25 kbar, whereas the rest of the solid line is a second-order-polynomial least-squares fit through the remaining data. From the measurements for these two samples,  $\Delta^G_{111}$  is found to be

$$(0.86 \pm 0.03) |T| \text{ meV (800°C sample)}$$

and

$$(0.82 \pm 0.03) |T| \text{ meV (730°C sample)}.$$

The average value is  $(0.84 \pm 0.02) |T| \text{ meV}$ , which is very close to the splitting of the excited state of the  $G$  line for gallium in germanium  $(0.99 \pm 0.03) |T| \text{ meV}$ .<sup>42</sup> In fact, the behavior of  $\Delta^G_{111}$  for both copper and gallium in germanium is almost identical, thus supporting the conclusion that the splitting of the  $G$  line is due only to the excited-state splitting and not that of the ground state. This strongly reinforces the deduction made above that  $\Delta'_{111} = 0$ . Note that the splittings of the various single-acceptor states are sensitive to the details of their wave functions.<sup>17,42</sup> One expects the wave function of the  $\Gamma_8$

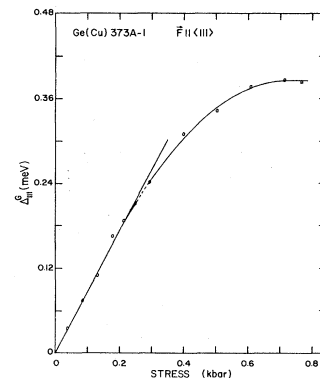


FIG. 15. Stress dependence of the splitting ( $\Delta^G_{111}$ ) of the single-hole excited state of the  $G$  line of neutral copper in germanium for  $F_{\parallel}\langle 111 \rangle$ . Copper diffused at 800°C;  $N_{\text{Cu}} = 1.32 \times 10^{16} \text{ cm}^{-3}$ .

ground state of a triple acceptor to be quite different from that of the single acceptor and thus, although surprising, it is not unreasonable that  $\Delta'_{111}=0$ .

It is now possible to examine the polarization characteristics of the components with a view to determining  $u_G$ . Under the condition that  $\Delta'_{111}=0$ , the energy level and transition scheme for  $F||\langle 111 \rangle$  (Refs. 17 and 18) becomes such that the six substates of the excited state collapse into two substates while the ground state undergoes no splitting. When the ordering of the substates of both the ground state and the  $\{\Gamma_8 \times \Gamma_8\} \times \Gamma_8$  excited state has been chosen to be consistent with the single acceptor scheme for the case of the  $G$  line,<sup>10,11,42</sup> it is predicted for neutral copper that only two  $G$  components be observed, each in both polarizations, in complete agreement with the experimental observations. When an attempt is made, however, to deduce the value of  $u_G$  from the relative intensities of these components inconsistencies arise. For example, in order that  $G_2$  be essentially zero at low stress (see Fig. 12), a value of two is required for  $u_G$ ,<sup>16</sup> whereas, theoretically,  $u_G$  is restricted to lie in the range zero to one.<sup>49</sup> That no agreement is found between the observed relative intensities and those predicted by the model for the  $G$  line is not surprising as no satisfactory assignment was found for the excited state of the  $G$  line for the other case already discussed, i.e.,  $F||\langle 100 \rangle$ .

### 3. Applied force along a $\langle 110 \rangle$ axis

In principle, the parameters which determine the splittings and relative intensities of a given spectral line can be obtained from observations with  $F||\langle 100 \rangle$  and  $\langle 111 \rangle$ . It is of value, however, and under special circumstances sometimes essential, to investigate the spectral behavior for an arbitrary direction of compression. The splitting of a given  $\Gamma_8$  for a single acceptor for any direction of applied force can be expressed in terms of the corresponding splittings for  $F||\langle 100 \rangle$  and  $F||\langle 111 \rangle$  [see Ref. 50, Eq. (15)]; this expression becomes quite simple for  $F||\langle 110 \rangle$ .<sup>49</sup> Relative intensities for a given transition under this latter direction of force for single acceptors have also been derived.<sup>49</sup> Equivalent expressions for both the splittings and relative intensities of a given line for  $F||\langle 110 \rangle$  have been determined for the triple acceptor.<sup>17,18</sup>

Typical spectra of neutral copper impurity in germanium with  $F||[110]$  are shown in Fig. 16 for a sample quenched from 730°C, where  $\mathbf{k}$ , the direction of light propagation, is parallel to  $[1\bar{1}0]$ . In Fig. 17 the energies of the various stress-induced components of the  $B$ ,  $C$ ,  $D$ , and  $G$  lines are plotted as a function of stress for this sample. The stress dependence of the  $G$  components for a sample quenched from 800°C has also been studied and it was found that at the highest stresses used, the  $G_1$  and  $G_2$  components exhibited further splittings. The solid lines in Fig. 17 are linear least-squares fits through the data for the various stress-induced components, whereas the dashed curves are simply aids to the eye.

A characteristic feature of the above spectra is that, under stress, each of the  $B$ ,  $C$ ,  $D$ , and  $G$  lines splits into three components. At moderate stress, the energies of the

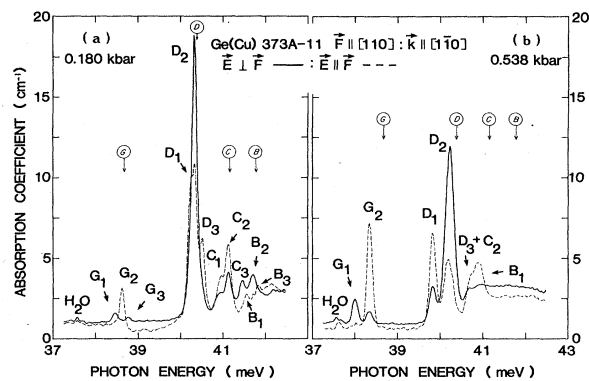


FIG. 16. Effect of  $F||[110]$  and  $\mathbf{k}||[1\bar{1}0]$  on the absorption spectrum of neutral copper in germanium at stresses of (a) 0.180 and (b) 0.538 kbar. Here  $\mathbf{k}$  is the propagation vector of the radiation. Liquid helium used as coolant. Copper diffused at 730°C;  $N_{Cu}=4.7 \times 10^{15} \text{ cm}^{-3}$ .

$B_1$ ,  $C$ 's, and  $G_2$  components exhibit nonlinear behavior. It is interesting to note that the onset of this nonlinear behavior and that of the corresponding behavior of the  $G$  components for  $F||\langle 111 \rangle$  occurs at almost the same stress (compare Figs. 14 and 17). Moreover, with increasing stress, the energy of the  $G_2$  component appears to follow the same stress dependence as that of  $G_1$ , along with a dramatic enhancement in its intensity accompanied by a significant decrease in the intensity of the  $D_2$  component. This behavior for  $G_2$  is almost identical to that of the  $G_2$  component for  $F||\langle 111 \rangle$ . Another feature is that, as already mentioned, at higher stress both the  $G_1$  and  $G_2$  components for the 800°C sample appear to split into two subcomponents. For the 730°C sample, these splittings are not observed although there is a slight broadening. It should be mentioned that similar splittings have been observed for some of the stress-induced components of lithium-oxygen donor complexes in silicon.<sup>52</sup> This has been attributed to an orientational degeneracy of this complex with the donors having axes along  $\langle 100 \rangle$  directions and consequently giving a symmetry lower than that of  $T_d$ . These subcomponents have been observed for this

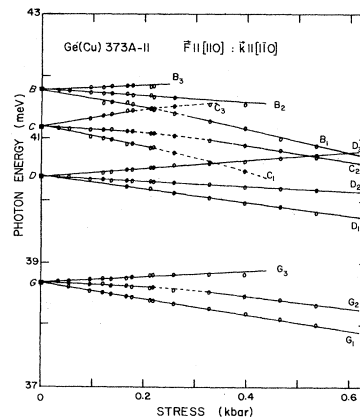


FIG. 17. Stress dependence of the energies of the components of the  $B$ ,  $C$ ,  $D$ , and  $G$  lines of neutral copper in germanium for  $F||[110]$  and  $\mathbf{k}||[1\bar{1}0]$  for the sample of Fig. 16.

TABLE IV. Splittings (in meV) of the ground and excited states of neutral copper in germanium for  $F||\langle 110 \rangle$ . (All entries are to be multiplied by  $|T|$ ;  $T$  is the stress in kbar.)

Splittings <sup>a</sup>		Sample	No. 11 (730°C)	No. 3 (800°C)
$\Delta'_{110}$	$(\epsilon_{G_3} - \epsilon_{G_1})$		1.66±0.05	1.62±0.02
	$(\epsilon_{D_3} - \epsilon_{D_1})$		1.71±0.03	
	$(\epsilon_{C_3} - \epsilon_{C_1})$		1.61±0.03	
$\Delta^D_{110}$	$(\epsilon_{D_2} - \epsilon_{D_1})$		0.59±0.03	
$\Delta^G_{110}$	$(\epsilon_{G_2} - \epsilon_{G_1})$		0.72±0.04	0.75±0.02

<sup>a</sup>The average values of the splittings are  $\Delta'_{110} = (1.65 \pm 0.05) |T|$  meV,  $\Delta^D_{110} = (0.59 \pm 0.03) |T|$  meV, and  $\Delta^G_{110} = (0.74 \pm 0.02) |T|$  meV.

complex with  $F||\langle 110 \rangle$  or  $F||\langle 100 \rangle$ , which supports the proposed model. For neutral copper, the additional splittings for the  $G$  components are not observed for  $F||\langle 100 \rangle$  or  $F||\langle 111 \rangle$ , which appears to eliminate the possibility of orientational degeneracy. Also, these additional splittings have not been observed for the  $D$  components for  $F||\langle 110 \rangle$  although, again, a slight broadening occurs similar to that for the  $G$  components [see Fig. 16(b)]. However, such a broadening could also be due to either inhomogeneity in the applied stress or overlapping of components associated with other lines. Another possibility is that the behavior of the two final substates associated with the two superimposed transitions comprising a given component undergo different interactions, as mentioned above and thus causing an additional splitting. This latter effect has not been seen for the other two orientations.

If one follows the approach for interpreting the results for  $F||\langle 100 \rangle$  and  $F||\langle 111 \rangle$ , where the ground state is assumed to be a  $\Gamma_8$  state, then a common splitting, the ground-state splitting, should be observed among the components of the various lines. In Table IV this common splitting, designated  $\Delta'_{110}$ , is given and is derived from the components of each of the  $C$ ,  $D$ , and  $G$  lines. The average of these three values is also given in this table. As the number of data points for a given line was insufficient to span the range of stress covered in the measurement and since the value obtained for  $\Delta'_{110}$  from each line is essentially the same, a composite plot of the data for all three lines was made<sup>17</sup> for the 730°C sample. In those cases where two or three of the lines give separate values for  $\Delta'_{110}$  an average was used; this is designated as  $\bar{\Delta}'_{110}$ .<sup>17</sup> The slope of the least-squares fit to these data gives a value of  $(1.62 \pm 0.02) |T|$  meV for  $\bar{\Delta}'_{110}$ . This value compares very favorably with the result shown in Table IV for  $\Delta'_{110}$  obtained from the data of the 800°C sample for the splitting of the  $G$  line alone, viz., the energy spacing of  $G_1$  and  $G_3$ .

Just as for single-hole acceptors,<sup>49</sup> a relation exists between  $\Delta'_{100}$ ,  $\Delta'_{111}$ , and  $\Delta'_{110}$ .<sup>13,14</sup> This relationship is

$$\Delta'_{110} = \frac{1}{2} [(\Delta'_{100})^2 + 3(\Delta'_{111})^2]^{1/2}. \quad (1)$$

Since for neutral copper  $\Delta'_{111}$  is interpreted to be zero, this relation then becomes simply

$$\Delta'_{110} = \frac{1}{2} \Delta'_{100}.$$

From the results obtained for  $\Delta'_{100}$  this yields

$$\Delta'_{110} = (1.59 \pm 0.04) |T| \text{ meV},$$

in excellent agreement with the observed result (see Table IV) and appears to confirm that  $\Delta'_{111} = 0$ .

The excited-state splitting for the  $D$  and  $G$  lines can be determined from the energy spacings  $\epsilon_{D_2} - \epsilon_{D_1}$  and  $\epsilon_{G_2} - \epsilon_{G_1}$ , respectively. For the case of the  $G$  line this choice for the excited-state splitting is justifiable as  $\epsilon_{G_3} - \epsilon_{G_2}$  is equal to  $\epsilon_{G_2} - \epsilon_{G_1}$  within the experimental errors, and, also, components  $G_1$  and  $G_2$  are those which survive at the highest stress and thus must arise from the lower ground-state sublevel. The values of  $\Delta^G_{110}$  are given in Table IV. These agree well with the value of  $(0.76 \pm 0.04) |T|$  meV obtained from an expression of the same form as Eq. (1), utilizing the results obtained for  $\Delta'_{111}$  and  $\Delta'_{100}$ . From the experimental results, it has not been possible to decide, unambiguously, that  $\Delta^D_{110} = \epsilon_{D_2} - \epsilon_{D_1}$  since all three  $D$  components are still observed up to the highest stress used. This assignment has been made on the basis of  $\Delta^D_{110} = (0.66 \pm 0.02) |T|$  meV predicted from the experimental results for  $\Delta^D_{100}$  and  $\Delta^D_{111}$ . This value is much closer to the observed spacing  $\epsilon_{D_2} - \epsilon_{D_1} = (0.59 \pm 0.03) |T|$  meV than to the spacing  $\epsilon_{D_3} - \epsilon_{D_2}$ , the only other choice for  $\Delta^D_{110}$ , determined to be  $(1.03 \pm 0.05) |T|$  meV from the data of Fig. 17.

A summary is given in Table V of the experimental splittings of the ground state and the excited states of  $D$  and  $G$  for the three orientations investigated. Also included are the predicted values for the splittings for  $F||\langle 110 \rangle$  (see column 4), based on Eq. (1).

The relative intensities of the components of a  $\Gamma_8 \rightarrow \Gamma'_8$  single acceptor transition for  $F||\langle 110 \rangle$  become as simple as for the other two directions of compression if there is no splitting of both the ground state and the excited state for either  $F||\langle 100 \rangle$  or  $F||\langle 111 \rangle$ . In fact, for  $\Delta'_{111} = \Delta^D_{111} = 0$ , the calculated relative intensities for  $F||[110]$ ,  $k||[1\bar{1}0]$  are identical to those for  $F||\langle 100 \rangle$  except the polarizations are interchanged, i.e., the  $E_{||}$  components for  $F||\langle 110 \rangle$  have the same relative intensities as the  $E_{\perp}$  components for  $F||\langle 100 \rangle$  (see Table XVIII of Ref. 49) and vice versa. Because of the correspondence between the predicted results for the single and triple ac-

TABLE V. Summary of splittings (in meV) of the ground and excited states of neutral copper in germanium for  $F_{||}\langle 100 \rangle$ ,  $F_{||}\langle 111 \rangle$ , and  $F_{||}\langle 110 \rangle$ . (All entries are to be multiplied by  $|T|$ ;  $T$  is the stress in kbar.)

Splittings	Direction of stress	$F_{  }\langle 100 \rangle$	Experimental $F_{  }\langle 111 \rangle$	$F_{  }\langle 110 \rangle$	Predicted <sup>a</sup> $F_{  }\langle 110 \rangle$
$\Delta'_{hkl}$		$3.17 \pm 0.08$	$\sim 0^b$	$1.62 \pm 0.02^c$	$1.59 \pm 0.04$
$\Delta^D_{hkl}$		$1.32 \pm 0.03$	$\sim 0^b$	$0.59 \pm 0.03$	$0.66 \pm 0.02$
$\Delta^G_{hkl}$		$0.46 \pm 0.11$	$0.84 \pm 0.03$	$0.73 \pm 0.04$	$0.76 \pm 0.04$

<sup>a</sup>The predicted values for  $F_{||}\langle 110 \rangle$  are based on the experimental values of  $\Delta_{100}$  and  $\Delta_{111}$  and Eq. (1).

<sup>b</sup>No measurable splitting for the  $D$  line (see text).

<sup>c</sup>The value given here is  $\bar{\Delta}'_{110}$  (see text).

ceptor, this simplification is carried over to the present case. Thus the model predicts that the intensity pattern of the  $E_{||}$  components for the  $D$  line for  $F_{||}\langle 110 \rangle$ ,  $\mathbf{k}_{||}\langle 1\bar{1}0 \rangle$  should be identical to that observed in  $E_{\perp}$  for  $F_{||}\langle 100 \rangle$  and vice versa. A comparison between the spectra of  $F_{||}\langle 100 \rangle$  (see Figs. 3 and 4) and those for  $F_{||}\langle 110 \rangle$  (see Fig. 16) shows that this prediction is clearly not borne out. This is not understood.

For the  $G$  components, little can be said about their intensities with  $F_{||}\langle 110 \rangle$  since the intensity parameters  $u_G$  and  $v_G$  could not be extracted from the experimental data. Some simplification of the expressions for these intensities can be accomplished since  $\Delta'_{111}=0$ , however, little purpose is served in pursuing this, at this time.

#### D. Deformation potential constants and intensity parameters

The deformation potential constants for the different energy states can be obtained from the experimental values of the  $\Delta$ 's and the theoretical expressions for these.<sup>16-18</sup> The values of the compliance coefficients,  $s_{11}$ ,  $s_{12}$ , and  $s_{44}$ , used in extracting the deformation-potential constants have been taken from Fine.<sup>53</sup> The results obtained are given in Table VI. Also given in this table, for comparison, are the corresponding deformation-potential constants for gallium<sup>52</sup> and singly-ionized zinc<sup>9,10,54</sup> in germanium. The deformation-potential constants of the single-hole acceptor states have been evaluated from effective-mass wave functions<sup>17,42</sup> and the experimental

values of the valence-band deformation-potential constants.<sup>55</sup> One set of these is shown in column 4 of Table VI.

It should be noted that the sign of  $b'$  for neutral copper is opposite to that of the single acceptors, gallium and singly-ionized zinc. From the equations developed for neutral copper,<sup>17,18</sup> this is expected when the model used is applied directly taking into account, as has been done, the experimentally observed ordering of the stress-induced substates of single acceptors. This correlation has also been used to specify the signs of the other deformation-potential constants of neutral copper.

The relative intensity parameters which have been extracted from the experimental data for copper in germanium are  $u_D=0.22$  and  $v_D=0.3$ . These values are to be compared with  $\sim 0.1$  and  $\sim 0.2$ , respectively, for boron in germanium<sup>43</sup> and 0.23 and 0.25, respectively, for singly-ionized zinc in germanium.<sup>6</sup> Calculated values of these two parameters for shallow acceptors in germanium are 0.19 and 0.37, respectively.<sup>42</sup>

#### IV. CONCLUDING REMARKS

The group-theoretical analysis<sup>16-19</sup> used to understand the present group-I results has been developed on the basis of the self-consistent-field approximation. In this model, the residual Coulomb interactions among the holes (hole-hole coupling) is assumed negligible since no splittings for the excitation lines of neutral copper in germanium have been observed at zero stress. Within the limits of this ap-

TABLE VI. Deformation potential constants for acceptors in germanium (in units of eV). [(Compliance coefficients of germanium (Ref. 53) used were  $s_{11}=9.585 \times 10^{-13}$  cm<sup>2</sup>/dyn,  $s_{12}=-2.609 \times 10^{-13}$  cm<sup>2</sup>/dyn, and  $s_{44}=14.542 \times 10^{-13}$  cm<sup>2</sup>/dyn.)]

Deformation-potential constant	Acceptor	Cu <sup>a</sup>	Ga <sup>b</sup>	Zn <sup>c</sup>	Calculated <sup>d</sup>
$b'$		$1.30 \pm 0.03$	$-1.33 \pm 0.03$	$-0.75 \pm 0.02$	$-1.15$
$d'$		$\sim 0$	$-2.91 \pm 0.06$	$-2.32 \pm 0.09$	$-2.53$
$b'_D$		$0.54 \pm 0.01$	$0.60 \pm 0.10$	$0.65 \pm 0.02$	$0.46$
$d'_D$		$\sim 0$	$<  0.06 $	$0.15 \pm 0.03$	$0.36$
$b'_G$		$0.19 \pm 0.05$	$0.213 \pm 0.007$		$0.25$
$d'_G$		$-1.00 \pm 0.04$	$-1.10 \pm 0.06$	$-1.45 \pm 0.09$	$-1.12$

<sup>a</sup>See text.

<sup>b</sup>See Ref. 42.

<sup>c</sup>See Refs. 9, 10, and 54.

<sup>d</sup>See Refs. 17 and 42.

proximation, it is shown that triple acceptors have a  $\Gamma_8$  ground state and more complex excited states. The predicted spectral behavior of a triple acceptor on this model is almost identical to that of a single acceptor, the only difference being that, in general, each stress-induced component of a triple-acceptor absorption line is compounded of two transitions one from each substate of the ground state.

The experimental results presented show that the spectra of neutral copper in germanium under stress are generally of simple structure and are indeed similar to those observed previously for single acceptors. This simplicity appears to confirm the assumption made that the ground-state splitting is replicated in the excited state.<sup>16-18</sup> A comparison of the spectrum in Fig. 3 for neutral copper and that reported by Jones and Fisher<sup>41</sup> for thallium in germanium illustrates the predicted similarity. Furthermore, the above predictions are borne out by the fact that the splitting obtained for each state of neutral copper for  $F||\langle 100 \rangle$  is almost equal to that for the corresponding state of gallium in germanium (see Table VI), although it is surprising that this should be so for the ground state. From the experimental results for  $F||\langle 111 \rangle$ , this similarity is again well illustrated by the stress dependence of  $\Delta_{111}^G$  (see Fig. 15); this is almost identical to that observed for gallium.<sup>42</sup> Furthermore, the characteristic feature,  $\Delta_{111}^D=0$ , observed for single acceptors is also found for the present case; this value is substantiated by the calculations,<sup>17,42</sup> particularly when the ratio  $|d'_D/d|=0.076$  is compared with that observed. In fact, the conclusion that  $\Delta'_{111}=0$  is the only quantitative difference between the splittings of the ground states and the excited states of the  $D$  and  $G$  lines of copper and gallium in germanium; this result is quite surprising. It might be expected that both  $\Delta'_{100}$  and  $\Delta'_{111}$  for copper should be different from those for gallium. However, since  $\Delta'_{100}$  is the same for these two acceptors, it is not at all clear why the  $\Delta'_{111}$  are so different. The excellent quantitative agreement between the splittings obtained for the various states with  $F||\langle 110 \rangle$  and the corresponding values predicted on the basis of the model using the results from the other two directions of  $F$  seems to confirm the interpretation of the experimental results up to this point.

Notwithstanding the above consistencies, there are several serious differences and discrepancies as has already been seen. The survival of the low-energy components for the various lines of the copper acceptor is in contrast with that reported for single acceptors.<sup>9-11,42</sup> This distinct feature cannot be explained on the grounds of the predicted energy-level scheme alone. In this scheme, as already mentioned, each stress-induced component is comprised of two transitions, one arising from each of the two ground substates. It is clear that the thermal depopulation effects on their own cannot be responsible for the complete disappearance of the high-energy components of the various lines at higher stress. However, the dramatic intensity variations of the components with the stress accompanied by a nonlinear stress dependence for some components and their intensity variation with temperature at a fixed stress strongly indicate that mixing among the associated final substates must be

taking place. This mixing might be an example of the interaction described by Chandrasekhar *et al.*<sup>50</sup> for acceptors in silicon and demonstrates that the components of a stronger line "feed" those of a weaker line, such as in the present case of the  $D$  and  $G$  lines for all the three orientations investigated.

This type of mixing taken together with the thermal depopulation effects, however, is still not adequate to explain the complete elimination of the  $G_3$  and  $G_4$  components since the  $G$  line is the weaker of the two. This leads to the possibility that either the  $G$  line "feeds" an even weaker line or there is still an additional mixing among the substates associated with a given spectral line; a possible example of such an additional mixing is reported by Duff *et al.* for singly-ionized zinc in germanium.<sup>11</sup> The only line which has not been observed for neutral copper, compared to the spectrum of a neutral single acceptor, is the  $E$  line which, however, is expected to lie outside the range of the present measurements, and since it corresponds to a  $1s \rightarrow 2s$  transition, is usually very weak.<sup>39</sup> It might be of value in the future to investigate the stress dependence of the  $E$  line not only for neutral copper but for other acceptors. It has been shown (see Fig. 27 of Ref. 17) that the rate of increase of  $G_1$  is almost the same as that of the decrease of  $G_3$  at low stress which strongly favors the possibility of the above additional mixing.

A particularly serious difficulty with the comparison between the experimental results and those predicted by the model is that the polarization behavior of the  $G$  components violates the selection rules for  $F||\langle 100 \rangle$ . An insufficient number of  $G$  components is observed to determine whether or not this same difficulty arises for  $F||\langle 111 \rangle$ . Unlike the  $G$  line, the behavior of the  $D$  line for  $F||\langle 100 \rangle$  appears to be in good agreement with the predictions. Also, for this orientation it has been concluded that the order of the substates of the ground state is the same as that of the final substates of the  $D$  line. Because of the ambiguity in the sign of the intensity parameter  $v_D$ , it was not possible to determine the order of the ground substates; these orderings have been chosen to be consistent with the single acceptor scheme for the  $D$  line. Irregardless of the success achieved in the understanding of the behavior of the  $D$  line for  $F||\langle 100 \rangle$  and  $F||\langle 111 \rangle$  the intensity parameters extracted from the former orientation fail to predict the intensity pattern observed with  $F||[110]$ ,  $k||[1\bar{1}0]$ . Finally, it is found that the compound shift of the center of gravity for the components of a given line are not equal for the three orientations chosen. The origin of this is not understood.

The discrepancies summarized above for the behavior of neutral copper indicate that the present model needs some modifications. It appears that including the type of mixing (interactions) mentioned above is not a sufficient modification to this model. It is difficult to understand that the small misorientation of the samples could lead to these discrepancies since the direction cosines parameter  $K$  [defined in Ref. 50, Eq. (15)] exhibits its extrema along the three orientations chosen for the present observations. In order to gain more information about neutral copper, it might be necessary to investigate orientations other than the three already used but in the same plane ( $\{110\}$  plane).

The general expression for the splitting of a  $\Gamma_8$  state<sup>50</sup> can give a guide as to which orientation is the most likely one for which four components of both the  $D$  and  $G$  lines might be observed. For example, the same splitting of a given  $\Gamma_8$  state obtained for  $F||\langle 110 \rangle$  can also be obtained with  $F||[11\bar{2}]$ , bearing in mind that the splittings should be more sensitive to misorientation for the latter crystallographic direction.

Additional information would be obtained presumably if either Zeeman or Piezo-Zeeman studies were made. This would, of course, not only involve an experimental investigation but also at least a similar group-theoretical analysis to that carried out for single acceptors.<sup>56</sup>

#### ACKNOWLEDGMENTS

The authors wish to thank Dr. A. D. Martin for assistance and advice regarding the data collection system, Dr. N. F. Kennon for x-ray verification of sample orienta-

tions, Dr. R. B. Roberts of the Division of Applied Physics, Commonwealth Scientific and Industrial Research Organisation (CSIRO), for technical assistance, Dr. A. J. Tavendale of the Australian Atomic Energy Commission for supplying pure single-crystal germanium, and the Department of Physics, Monash University, for reconstructing the detector cryostat. Thanks are also due to Professor A. K. Ramdas of Purdue University for a critical reading of the manuscript and to Dr. L. Eaves of the University of Nottingham for useful discussion. One of the authors (E.H.S) wishes to thank the University of Wollongong for a University Research Award held during most of the period of the research reported and also Cairo University for study leave during the course of the work. Another author (P.F.) wishes to thank the Department of Physics of Purdue University for hospitality during part of the writing of the manuscript. The work was supported by the Australian Research Grants Scheme and the University of Wollongong Research Grants Committee.

\*Present address: Bell Communications Research, Inc., Morristown, NJ 07960.

<sup>1</sup>For the most recent review of this field, see A. K. Ramdas and S. Rodriguez, *Rep. Prog. Phys.* **44**, 1297 (1981).

<sup>2</sup>H. Shenker, E. M. Swiggard, and W. J. Moore, *Trans. Metall. Soc. AIME* **239**, 347 (1967).

<sup>3</sup>J. W. Cross, L. T. Ho, A. K. Ramdas, R. Sauer, and E. E. Haller, *Phys. Rev. B* **28**, 6953 (1983).

<sup>4</sup>P. Fisher and H. Y. Fan, *Phys. Rev. Lett.* **5**, 195 (1960).

<sup>5</sup>W. J. Moore, *Solid State Commun.* **3**, 385 (1965).

<sup>6</sup>P. Fisher, R. L. Jones, A. Onton, and A. K. Ramdas, *J. Phys. Soc. Jpn. Suppl.* **21**, 224 (1966).

<sup>7</sup>R. L. Jones, Ph.D. thesis, Purdue University, 1968 (unpublished).

<sup>8</sup>W. J. Moore, *J. Phys. Chem. Solids* **32**, 93 (1971).

<sup>9</sup>F. Barra, P. Fisher, and S. Rodriguez, *Phys. Rev. B* **7**, 5285 (1973).

<sup>10</sup>N. R. Butler and P. Fisher, *Phys. Rev. B* **13**, 5465 (1976).

<sup>11</sup>K. J. Duff, P. Fisher, and N. R. Butler, *Aust. J. Phys.* **33**, 73 (1980).

<sup>12</sup>R. A. Chapman and W. G. Hutchinson, *Solid State Commun.* **3**, 293 (1965); *Phys. Rev.* **157**, 615 (1967); R. A. Chapman, W. G. Hutchinson, and T. L. Estles, *Phys. Rev. Lett.* **17**, 132 (1966).

<sup>13</sup>B. Pajot and Y. Darvot, *Phys. Lett.* **21**, 512 (1966).

<sup>14</sup>N. R. Butler and P. Fisher, *Phys. Lett.* **47A**, 391 (1974).

<sup>15</sup>E. E. Haller, W. L. Hansen, and F. S. Goulding, *Adv. Phys.* **30**, 93 (1981).

<sup>16</sup>E. H. Salib, K. J. Duff, P. Fisher, and P. E. Simmonds, *Solid State Commun.* **44**, 81 (1982).

<sup>17</sup>E. H. Salib, Ph.D. thesis, University of Wollongong, 1982 (unpublished).

<sup>18</sup>E. H. Salib and K. J. Duff (unpublished).

<sup>19</sup>K. J. Duff, *Aust. J. Phys.* **35**, 401 (1982); K. J. Duff and E. H. Salib, *ibid.* **36**, 485 (1983); see also G. Kirczenow, *Can. J. Phys.* **55**, 1787 (1977).

<sup>20</sup>C. S. Fuller, J. D. Struthers, J. A. Ditzenberger, and K. B. Wolfstirn, *Phys. Rev.* **93**, 1182 (1954).

<sup>21</sup>V. I. Fistul', A. Yakovenko, and E. A. Shelonin, *Fiz. Tverd Tela (Leningrad)* **22**, 31 (1980) [*Sov. Phys.—Solid State* **22**, 17 (1980)].

<sup>22</sup>A. Smakula and V. Sils, *Phys. Rev.* **99**, 1744 (1955).

<sup>23</sup>V. J. Tekippe, H. R. Chandrasekhar, P. Fisher, and A. K. Ramdas, *Phys. Rev. B* **6**, 2348 (1972).

<sup>24</sup>N. R. Butler, Ph.D. thesis, Purdue University, 1974 (unpublished).

<sup>25</sup>Model No. 5381, Morehouse Instruments Co., 1742 Sixth Avenue, York, Pennsylvania.

<sup>26</sup>SPEX Industries, Inc., Metuchen, New Jersey.

<sup>27</sup>A. R. H. Cole, *Tables of Wavenumbers for the Calibration of Infrared Spectrometers* (Pergamon, Oxford, 1977).

<sup>28</sup>Model No. 221-5573, Perkin-Elmer Corp., Main Avenue, Norwalk, Connecticut.

<sup>29</sup>A. Mitsuishi, Y. Yamada, S. Fujita, and H. Yoshinaga, *J. Opt. Soc. Am.* **50**, 433 (1960).

<sup>30</sup>Santa Barbara Research Center, Goleta, California.

<sup>31</sup>Andonian Cryogenics Inc., Massachusetts, and the Department of Physics, Monash University, Clayton, Victoria, Australia.

<sup>32</sup>Model No. 124A, Princeton Applied Research Corp., Princeton, New Jersey.

<sup>33</sup>Model No. AD-2008, Analog Devices, Norwood, Massachusetts.

<sup>34</sup>Model No. HP-9825A, Hewlett-Packard Co., Loveland, Colorado.

<sup>35</sup>Data General Corporation, Southboro, Massachusetts.

<sup>36</sup>Rockwell Microelectronic Devices, Anaheim, California.

<sup>37</sup>Model No. 130-P60, Zeta Research Inc., Lafayette, California.

<sup>38</sup>S. J. Fray, F. A. Johnson, J. E. Quarrington, and N. Williams, *Proc. Phys. Soc.* **85**, 153 (1965).

<sup>39</sup>R. L. Jones and P. Fisher, *J. Phys. Chem. Solids* **26**, 1125 (1965).

<sup>40</sup>A. F. Polupanov and Sh. M. Kogan, *Fiz. Tekh. Poluprovodn.* **13**, 2338 (1979) [*Sov. Phys.—Semicond.* **13**, 1368 (1979)].

<sup>41</sup>R. L. Jones and P. Fisher, *Solid State Commun.* **2**, 369 (1964); *Phys. Rev. B* **2**, 2016 (1970).

<sup>42</sup>A. D. Martin, P. Fisher, C. A. Freeth, E. H. Salib, and P. E. Simmonds, *Phys. Lett.* **99A**, 391 (1983).

<sup>43</sup>H. P. Soepangkat and P. Fisher, *Phys. Rev. B* **8**, 870 (1973).

<sup>44</sup>A. G. Kazanskii, P. L. Richards, and E. E. Haller, *Solid State Commun.* **24**, 603 (1977).

<sup>45</sup>A. Onton, P. Fisher, and A. K. Ramdas, *Phys. Rev. Lett.* **19**, 781 (1967).

<sup>46</sup>K. Arya and S. S. Jha, *Phys. Rev. B* **14**, 4727 (1976).

- <sup>47</sup>P. Norton and H. Levinstein, *Phys. Rev. B* **6**, 470 (1972).
- <sup>48</sup>K. Colbow, *Can. J. Phys.* **41**, 1801 (1963).
- <sup>49</sup>S. Rodriguez, P. Fisher, and F. Barra, *Phys. Rev. B* **5**, 2219 (1972).
- <sup>50</sup>H. R. Chandrasekhar, P. Fisher, A. K. Ramdas, and S. Rodriguez, *Phys. Rev. B* **8**, 3836 (1973).
- <sup>51</sup>E. E. Haller, B. Joos, and L. M. Falicov, *Phys. Rev. B* **21**, 4729 (1980).
- <sup>52</sup>C. Jagannath and A. K. Ramdas, *Phys. Rev. B* **23**, 4426 (1981).
- <sup>53</sup>M. E. Fine, *J. Appl. Phys.* **26**, 862 (1955).
- <sup>54</sup>K. J. Duff, P. Fisher, and N. R. Butler (unpublished).
- <sup>55</sup>J. C. Hensel and K. Suzuki, *Phys. Rev. B* **9**, 4219 (1974).
- <sup>56</sup>A. K. Bhattacharjee and S. Rodriguez, *Phys. Rev. B* **6**, 3836 (1972).